 doi:10.20944/preprints201708.0009.v2

Subterranean Karst Environments as a Global Sink for Atmospheric Methane

Kevin D. Webster[1,2], Agnieszka Drobniak[3], Giuseppe Etiope[4,5], Maria Mastalerz[3], Peter E. Sauer[6] and Arndt Schimmelmann[6]

[1]School of Natural Resources and the Environment, University of Arizona, 1064 E Lowell St, Tucson, Arizona 85721, USA

[2]Department of Ecology and Evolutionary Biology, University of Arizona, 1041 E Lowell St, Tucson, Arizona 85721, USA.

[3]Indiana Geological Survey, Indiana University, 611 North Walnut Grove Ave., Bloomington, Indiana 47405, USA.

[4] Istituto Nazionale di Geofisica e Vulcanologia, Sezione Roma 2, Italy.

[5] Faculty of Environmental Science and Engineering, Babes-Bolyai University, Cluj-Napoca, Romania.

[6] Department of Earth and Atmospheric Sciences, Indiana University, 1001 E 10th St. Bloomington, IN 47405, USA.

* corresponding author: kevdwebs@email.arizona.edu; telephone: 520-621-2539

Keywords: cave; greenhouse gas; karst; methane; methanogenesis; methanotrophy

 doi:10.20944/preprints201708.0009.v2

Abstract

The air in subterranean karst cavities is often depleted in methane (CH_4) relative to the atmosphere. Karst is considered a potential sink for the atmospheric greenhouse gas CH_4 because its subsurface drainage networks and solution-enlarged fractures facilitate atmospheric exchange. Karst landscapes cover about 14 % of earth's continental surface, but observations of CH_4 concentrations in cave air are limited to localized studies in Gibraltar, Spain, Indiana (USA), Vietnam, Australia, and by incomplete isotopic data. To test if karst is acting as a global CH_4 sink, we measured the CH_4 concentrations, $\delta^{13}C_{CH_4}$, and $\delta^{2}H_{CH_4}$ values of cave air from 33 caves in the USA and three caves in New Zealand. We also measured CO_2 concentrations, $\delta^{13}C_{CO_2}$, and radon (Rn) concentrations to support CH_4 data interpretation by assessing cave air residence times and mixing processes. Among these caves, 35 exhibited subatmospheric CH_4 concentrations in at least one location compared to their local atmospheric backgrounds. CH_4 concentrations, $\delta^{13}C_{CH_4}$, and $\delta^{2}H_{CH_4}$ values suggest that microbial methanotrophy within caves is the primary CH_4 consumption mechanism as the atmosphere exchanges with subsurface air. The $\delta^{13}C_{CH_4}$ and $\delta^{2}H_{CH_4}$ values observed in cave air provide evidence for incomplete oxidation by methanotrophy. Only 5 locations from 3 caves showed elevated CH_4 concentrations compared to the atmospheric background and could be ascribed to local CH_4 sources from sewage and outgassing swamp water. Several associated $\delta^{13}C_{CH_4}$ and $\delta^{2}H_{CH_4}$ values point to carbonate reduction and acetate fermentation as biochemical pathways of limited methanogenesis in karst environments and suggest that these pathways occur in the environment over large spatial scales. Our data show that karst environments function as a global CH_4 sink.

 doi:10.20944/preprints201708.0009.v2

1. Introduction

Atmospheric methane (CH_4) is a greenhouse gas and its concentration is increasing in the atmosphere (Dlugokencky et al., 2011; Sussmann et al., 2012; Ciais et al., 2013). The increase in atmospheric CH_4 is due to an imbalance between CH_4 sources and sinks. Anthropogenic and natural sources combine to contribute about 680 Tg a^{-1} of CH_4 to the atmosphere while reactions with hydroxyl (·OH) and chlorine radicals in the troposphere and stratosphere remove about 600 Tg a^{-1} (Kirschke et al., 2013). Methanotrophic consumption in soils removes 30 Tg a^{-1} (Kirschke et al., 2013). The present globally averaged CH_4 concentration is 1.87 ppmv which is 2.5 times higher than preindustrial levels (Nisbet et al., 2016). Despite improvements in estimating individual sources and sinks of atmospheric CH_4, the associated errors remain large (Kirschke et al., 2013). Recent studies suggest that caves may act as an additional CH_4 sink (Mattey et al., 2013; Fernandez-Cortes et al., 2015; McDonough et al., 2016; Webster et al., 2016; Lennon et al., 2017).

Caves and associated karst landscapes may be an important overlooked sink for atmospheric CH_4 because they are estimated to cover as much as 10 to 20 % of the continental surface with more precise estimates suggesting about 13.8 % (Palmer, 1991; Ford and Williams, 2007). Karst landscapes are frequently associated with the chemical dissolution of limestones, but can form in any soluble rock body. The resulting caves, solution-enlarged fractures, and internal drainage networks that function to transport mass from high elevations to low elevations also allow for subsurface-surface atmospheric exchange (Kowalczk and Froelich, 2010; Garcia-Anton et al., 2014). The total volume and surface area of karst conduits able to interact with the atmosphere is unknown, in part due to small fractures and the difficulty of imaging the subsurface with geophysical methods. Karst caves, due to their accessibility, provide opportunities for non-invasive, *in-situ* analyses and sampling.

Preprints (www.preprints.org) | NOT PEER-REVIEWED | Posted: 29 October 2017 doi:10.20944/preprints201708.0009.v2

Cave and karst landscapes form in two common ways, each of which influences karst's capacity to act as a CH_4 sink. Epigenic karst forms through the interaction of limestone with carbonic acid derived from the dissolution of atmospheric and soil CO_2 into surface waters. By contrast, hypogenic caves form when corrosive water from deep sources migrates into and dissolves limestone bedrock. Epigenic caves are more widespread, and atmospheric to subatmospheric CH_4 concentrations of 1.8 ppmv to < 0.1 ppmv have been observed in these settings (Mattey et al., 2013; Fernandez-Cortes et al., 2015; McDonough et al., 2016; Webster et al., 2016; Lennon et al., 2017). For comparison, in some hypogenic caves elevated CH_4 concentrations from 2 ppmv to 1 % have been observed in association with CH_4-rich springs or seeps related to fluid migration from deep hydrocarbon-bearing sedimentary rocks, i.e. seepage processes that are widespread on Earth (Sarbu et al., 1996; Hutchens et al., 2004; Jones et al., 2012; Webster et al., 2017). The dominance of epigenic karst suggests that karst is likely functioning as a CH_4 sink at the global scale, but more observations are needed.

Different hypotheses have been put forward to explain the low CH_4 concentrations observed in epigenic cave air. The combination of subatmospheric CH_4 concentrations and the stable carbon isotopic ratio of CH_4 in the air of caves in Gibraltar led to the hypothesis that microorganisms were responsible for the removal of CH_4 (Mattey et al., 2013). In turn, low CH_4 concentrations in Spanish caves, in the presumed absence of CH_4-consuming (methanotrophic) bacteria, led to the hypothesis that CH_4 oxidation was induced by ions and ·OH generated by the radioactive decay of radon and daughter nuclides (Fernandez-Cortes et al., 2015). Since these initial observations, datasets from caves in Australia, the USA, and Vietnam have pointed towards methanotrophic CH_4 oxidation (McDonough et al., 2016; Webster et al., 2016; Lennon et al., 2017, Waring et al., 2017).

Preprints (www.preprints.org) | NOT PEER-REVIEWED | Posted: 29 October 2017 doi:10.20944/preprints201708.0009.v2

The chemical composition of cave air results from the mixing of the atmosphere and air from the overlying soils and epikarst. These processes should influence the CH_4 concentrations of cave air. Previous studies have shown that CH_4 concentrations have been inversely correlated with CO_2 concentrations in cave air (Mattey et al., 2013; Ferndandez-Cortes et al., 2015; McDonough et al., 2016; Webster et al., 2016). Cave air CO_2 concentrations are positively correlated with radon (Rn) concentrations and Rn is known to track cave air residence time (Cunningham and LaRock, 1991; Batiot-Guilhe et al., 2007; Kowalczk and Froelich, 2010; Mattey et al., 2010; Gregorič et al., 2011, 2014). Additionally, the stable C isotope composition of CO_2 ($\delta^{13}C_{CO_2}$), can track the sources of CO_2 in the environment. For example, $\delta^{13}C_{CO_2}$ values of −24 ‰ are associated with soil CO_2, while atmospheric CO_2 has $\delta^{13}C_{CO_2}$ values ranging from −8.5 ‰ to −10 ‰ (Amundson et al., 1998; Keeling et al., 2010; Peyraube et al., 2013). Thus CO_2, Rn, and $\delta^{13}C_{CO_2}$ in cave air can help determine the influence of cave air mixing processes on CH_4.

The stable C and H isotope compositions of CH_4 ($\delta^{13}C_{CH_4}$ and $\delta^{2}H_{CH_4}$) also provide tools for understanding the sources and sinks of CH_4 in caves because different CH_4 sources are associated with characteristic $\delta^{13}C_{CH_4}$ and $\delta^{2}H_{CH_4}$ values. For example, CH_4 produced from carbonate reduction has $\delta^{13}C_{CH_4}$ and $\delta^{2}H_{CH_4}$ values that range from −112 to −60 ‰ VPDB and from −350 to −100 ‰ VSMOW respectively (Whiticar, 1999). Atmospheric CH_4 has $\delta^{13}C_{CH_4}$ and $\delta^{2}H_{CH_4}$ values around −47.5 and −100 ‰ (Miller et al., 2002; Townsend-Small et al., 2012). The $\delta^{13}C_{CH_4}$ and $\delta^{2}H_{CH_4}$ values of CH_4 can also be altered through secondary processes such as oxidation and mixing. The oxidation pathways of CH_4 by methanotrophs or ·OH have fractionation factors that result in residual CH_4 having increased in $\delta^{2}H_{CH_4}$ values of 8.5 ‰ for every 1 ‰ increase in $\delta^{13}C_{CH_4}$ value and increases in $\delta^{2}H_{CH_4}$ values of 72 ‰ for every 1 ‰ increase in $\delta^{13}C_{CH_4}$

Preprints (www.preprints.org) | NOT PEER-REVIEWED | Posted: 29 October 2017 doi:10.20944/preprints201708.0009.v2

value, respectively (Feisthauer et al., 2011; Saueressig et al., 2001). Mixing between two different CH_4 sources creates a linear trend between the two members. Thus measuring the $\delta^{13}C_{CH_4}$ and $\delta^{2}H_{CH_4}$ of cave air should allow for the determination of cave air CH_4 sources.

The objective of the present work is to extend the karst CH_4 dataset and test the hypothesis that karst systems act as a CH_4 sink on a global scale. To this aim, we studied CH_4 concentration, $\delta^{13}C_{CH_4}$, and $\delta^{2}H_{CH_4}$ in cave air from 33 epigenic caves in the USA and three epigenic caves in New Zealand. CO_2, $\delta^{13}C_{CO_2}$, and Rn were also measured to support CH_4 data interpretation *via* assessing cave air residence times and mixing processes. Data analysis is focused on determining CH_4 concentrations, origin, mixing processes and isotopic fractionations.

2. Methods

2.1. Sampling and analyses

Air samples from 16 limestone or dolostone caves in the Appalachian fold and thrust belt, 17 limestone caves in gently warped intracratonic basins of the USA, and 3 caves from the North Island of New Zealand were collected over a timespan of roughly four years (Fig. 1; Table 1). Cave air was analyzed using *in-situ* methods and was further sampled for laboratory analysis. *In-situ* CH_4, CO_2, and Rn abundance analyses were carried out using a suite of instruments (Table 2). Discrete samples of cave air were collected in pre-evacuated 50-mL serum vials, in 1 to 3-L Tedlar® bags, or in 4-L glass bottles. CH_4 and CO_2 concentrations of discrete samples were measured *via* gas chromatography.

We assessed cave air mixing processes through the following techniques. A qualitative estimate on cave air residence time was obtained by comparing CH_4 to CO_2 concentrations at

Preprints (www.preprints.org) | NOT PEER-REVIEWED | Posted: 29 October 2017 doi:10.20944/preprints201708.0009.v2

individual locations in each cave. Additionally, we measured the Rn concentrations of caves 32 through 36 to assess the relationship between cave air residence time, CH_4 concentrations, and CO_2 concentrations. $\delta^{13}C_{CO_2}$ data were used to assess the sources of CO_2 and thus of air entering the caves. We also assessed the distance from each sampling location to cave entrances as another tool to understand cave air mixing processes.

CH_4 and CO_2 concentrations from discrete air samples were measured at Indiana University using a Varian 450 gas chromatograph (GC) (Varian – Agilent Technologies, Palo Alto, California). The GC was fitted with a flame ionization detector (FID) for CH_4 and a thermal conductivity detector (TCD) for CO_2. Standard gas mixtures from Air Liquide America Specialty Gasses LLC (Plumsteadville, Pennsylvania) were used for 3-point calibration curves to convert signals measured on the GC to concentrations. CH_4 standards measured on the GC had errors of ± 5 to ± 14 % of the reported concentrations. CH_4 concentrations are reported with the uncertainty associated with the standard curve unless the calculated uncertainty was ≤ 0.1 ppmv. Samples with calculated uncertainties ≤ 0.1 ppmv were assigned uncertainties of 0.1 ppmv based on replicate measurements. The uncertainty associated with standard curves for CO_2 concentrations varied from < ± 1 to 5 %. CO_2 concentrations were assigned uncertainties based on their associated standard curve.

The stable carbon isotope ratios of CH_4 and CO_2 and hydrogen stable isotope ratios of CH_4 were measured on a ThermoFinnigan Delta Plus XP mass spectrometer in the Stable Isotope Research Facility at Indiana University. Carbon stable isotope ratios are expressed as conventional $\delta^{13}C_{CH_4}$ and $\delta^{13}C_{CO_2}$ values in ‰ along the scale anchored to Vienna Pee Dee Belemnite (VPDB). Hydrogen stable isotope ratios are expressed as $\delta^{2}H_{CH_4}$ values in ‰ along the scale anchored to Vienna Standard Mean Ocean Water (VSMOW). CH_4 samples were measured in continuous-flow

Preprints (www.preprints.org) | NOT PEER-REVIEWED | Posted: 29 October 2017 doi:10.20944/preprints201708.0009.v2

mode using CH_4 preconcentration, cryofocusing (Miller et al., 2002), and a gas chromatography-oxidation/pyrolysis-isotope ratio mass spectrometer (GC-ox/pyr-IRMS) interface. Varying sample extraction times were used to isolate roughly 0.45 and 0.90 μmol of CH_4 prior to the introduction of the sample to the GC-ox/pyr-IRMS for analysis of $\delta^{13}C_{CH_4}$ and $\delta^{2}H_{CH_4}$ values, respectively. In-house CH_4 standards methane #3, methane #6, and methane ALM with $\delta^{13}C_{CH_4}$ and $\delta^{2}H_{CH_4}$ values of [+19.86 ± 0.05; +2.2 ± 1.2] ‰, [−39.40 ± 0.02; −153 ± 2] ‰, and [−58 ± 1; −272.2 ± 3.4] ‰ were used for 2-point normalizations. Errors associated with $\delta^{13}C_{CH_4}$ and $\delta^{2}H_{CH_4}$ values were calculated using a standard curve that accounted for the peak size of the measurement. Analytical repeatability of internal standards ranged from 0.14 to 0.6 ‰ for $\delta^{13}C_{CH_4}$ and from to 7 to 18 ‰ for $\delta^{2}H_{CH_4}$.

$\delta^{13}C_{CO_2}$ values were measured in continuous-flow mode using a GasBench II inlet (Tu et al., 2001). Measured $^{13}C/^{12}C$ ratios of CO_2 from cave air were converted to the VPDB scale using a single isotopically characterized in-house standard that has a value of 12.0 ± 0.2 ‰.

2.2 Data elaboration and quality control

In-situ measurements were preferentially used when statistically analyzing gas concentration data. When *in-situ* measurements were not available, concentrations measured on the GC were used in the statistical analyses. Samples and data were screened for quality control by comparing the samples with *in-situ* measurements and visual estimation of the volume of sample bags. If a sample bag had been shown to exhibit a leak for one analyte, data from that sample were discarded. CH_4 and CO_2 concentrations measured by both GC-FID and FTIR showed strong agreements ($GC(CO_2) = 0.92 \pm 0.04 * FTIR(CO_2) + 100 \pm 300$, $r^2 = 0.99$, $p = 5*10^{-19}$;

Preprints (www.preprints.org) | NOT PEER-REVIEWED | Posted: 29 October 2017 doi:10.20944/preprints201708.0009.v2

GC(CH_4) = 0.7 ± 0.2 * FTIR(CH_4) + 0.2 ± 0.2, r^2 = 0.62), and the stable isotopic composition of the samples was not related to their storage time ($\delta^{13}C_{CH_4}$ = 0.2 ± 0.3*day −47 ± 2, r^2 = 0.03, p = 0.32; $\delta^{2}H_{CH_4}$ = 0.03 ± 0.14*day −96 ± 11, r^2 = 0.005, p = 0.72; $\delta^{13}C_{CO_2}$ = −0.05 ± 0.16*day −19.9 ± 1.8, r^2 = 0.006, p = 0.57). In locations where more than one sample was taken with *in-situ* methods, the values of the samples were averaged. In total, 199 CH_4 concentrations, 192 CO_2 concentrations, 32 $\delta^{13}C_{CH_4}$ values, 26 $\delta^{2}H_{CH_4}$ values, and 60 $\delta^{13}C_{CO_2}$ values are reported in this study (Supplemental Tables 1, 2). All samples are reported with 95 % confidence intervals.

Three different modeling techniques were used to assess trace gas sources and sinks in the studied caves. Keeling plots were used to assess the possibility of a two end member mixing system affecting $\delta^{13}C_{CO_2}$. The stable isotopic composition of CO_2 entering the caves ($\delta^{13}C_s$) was assessed through equation 1

$$\delta^{13}C_s = (\delta^{13}C_m - F_{atm} * \delta^{13}C_{atm})\,(1 - F_{atm})^{-1} \quad (1)$$

where $\delta^{13}C_m$ is the $\delta^{13}C_{CO_2}$ of the sample, $\delta^{13}C_{atm}$ is the $\delta^{13}C_{CO_2}$ of the atmosphere, and F_{atm} is the fraction of atmospheric CO_2 in the CO_2 concentration of the sample (Peyraube et al., 2016). We used values of −10 ‰ for $\delta^{13}C_{atm}$ and 400 ppmv for the concentration of atmospheric CO_2.

Rayleigh distillation models were used as the theoretical basis to examine changes in the stable isotopic composition of CH_4 in cave air caused by methanotrophy or ·OH oxidation. The δ-value of an isotope system in a chemical compound of interest (e.g., CH_4) in cave air can be modeled as

$$\delta_c = (\delta_i + 1000)\, f^{(-\alpha + 1)} - 1000 \quad (2)$$

Preprints (www.preprints.org) | NOT PEER-REVIEWED | Posted: 29 October 2017 doi:10.20944/preprints201708.0009.v2

where δ_c is the instantaneous δ-value of a particular isotope system in cave air after partial consumption, δ_i is the initial δ-value of the isotope system in cave air, f is the fraction of the compound remaining, and α is the kinetic isotope fractionation factor (Mattey et al., 2013). α values of 1.018 and 1.1353 were used to model changes in $\delta^{13}C_{CH_4}$ and $\delta^{2}H_{CH_4}$ caused by methanotrophy (Coleman et al., 1981; Feisthauer et al., 2011). α values for changes in $\delta^{13}C_{CH_4}$ caused by methanotophy have been observed to range from 1.003 to 1.039 (Templeton et al., 2006; Feisthauer et al., 2011); 1.018 was selected based on observations of methanotrophy in soils and its similarity to the α value of 1.012 observed in St. Michael's Cave in Gibraltar (Feisthauer et al., 2011; Mattey et al., 2013). α values of 1.0039 and 1.294 were used to model changes in $\delta^{13}C_{CH_4}$ and $\delta^{2}H_{CH_4}$ values caused by ·OH oxidation (Saueressig et al., 2001). The initial stable isotopic composition of atmospheric CH_4 was modeled with a $\delta^{13}C_{CH_4} = -47.5$ ‰ (VPDB), and $\delta^{2}H_{CH_4} = -100$ ‰ (VSMOW) based on the work of Townsend-Small et al. (2012).

We examined the possibility of additional CH_4 sources entering the cave systems through forward modeling. We assumed that two different sources of microbially produced CH_4 contribute to cave air in addition to the atmosphere. We modeled CH_4 produced from acetate fermentation as S1 ($\delta^{13}C_{CH_4} = -49$ ‰ VPDB, $\delta^{2}H_{CH_4} = -325$ ‰ VSMOW) and from carbonate reduction as S2 ($\delta^{13}C_{CH_4} = -63$ ‰ VPDB, $\delta^{2}H_{CH_4} = -125$ ‰ VSMOW) respectively (Whiticar, 1999; Etiope and Sherwood Lollar, 2013). These sources were mixed with cave air both prior to and after partial theoretical methanotrophic oxidation. Methanotrophic oxidation was modeled with the aforementioned α values of 1.018 and 1.1353.

Preprints (www.preprints.org) | NOT PEER-REVIEWED | Posted: 29 October 2017 doi:10.20944/preprints201708.0009.v2

3. Results

Each of the 36 caves showed atmospheric to subatmospheric CH_4 concentrations in at least one location. Only five locations from three different caves showed elevated CH_4 concentrations relative to the atmosphere (Fig. 2, Supplemental Table 1). The CH_4 concentration in the atmosphere at study sites ranged from 1.8 ± 0.3 to 2.8 ± 0.7 ppmv. CH_4 concentrations in cave air ranged from ≤ 0.1 ± 0.1 ppmv to 5 ± 1 ppmv, and were generally observed to decrease with the distance from cave entrances (Fig. 3, Supplemental Table 1). Two thirds of the caves where three or more air measurements and distance data were recorded showed decreases in CH_4 concentration from cave entrances to interiors. For example, caves 7, 8, and 9 from Kentucky all showed progressive decreases in CH_4 concentration from about 2 ppmv at the entrance of the cave, down to zero or near zero ppmv in the more inner rooms (from 2 to 0 in caves 8 and 9 and from 1.9 to 0.3 ppmv in cave 7). Additionally, CH_4 concentrations were negatively correlated with CO_2 concentrations in cave air following an inverse power law relationship ($[CH_4] = 17.5[CO_2]^{-0.41}$, $r^2 = 0.26$) (Fig. 2). In the caves where Rn concentrations were measured, the average CO_2 concentration of cave air was correlated with the average Rn concentration of cave air ($[CO_2] = (1.42 \pm 0.09)[Rn] + 400 \pm 120$, $n = 4$, $r^2 = 0.99$, $p = 0.009$).

Values of $\delta^{13}C_{CO_2}$ in cave air ranged from −10.7 ± 0.4 to −23.81 ± 0.10 ‰. Analysis of $\delta^{13}C_{CO_2}$ values from samples with CO_2 concentrations above 600 ppmv showed that $\delta^{13}C_s$ ranging from −28 ‰ to −20 ‰ contributed to the composition of CO_2 in cave air. Pooled analysis of the CO_2 dataset shows that the average apparent source $\delta^{13}C_{CO_2}$ value is −23.3 ± 0.5 ‰ ($\delta^{13}C_{CO_2} = 4600\ [CO_2]^{-1} - 23.3 \pm 0.5$ ‰, $r^2 = 0.83$) (Fig. 4).

Preprints (www.preprints.org) | NOT PEER-REVIEWED | Posted: 29 October 2017 doi:10.20944/preprints201708.0009.v2

Values of $\delta^{13}C_{CH_4}$ and $\delta^{2}H_{CH_4}$ in cave air ranged from to −57.2 ± 0.6 to −27.1 ± 0.2 ‰ and −196 ± 10 to +2 ± 18 ‰, respectively. Keeling plots of $\delta^{13}C_{CH_4}$ did not suggest that a two end member model was an adequate fit for the system ($\delta^{13}C_{CH_4}$ vs. $[CH_4]^{-1}$: r^2 = 0.05, $\delta^{2}H_{CH_4}$ vs. $[CH_4]^{-1}$: r^2 = 0.12). Some cave air samples plotted near the theoretical relationship between $\delta^{13}C_{CH_4}$ values and CH_4 concentrations caused by methanotrophy (Fig. 5). However, many points fell below and to the left of the line representing the theoretical incomplete oxidation of atmospheric CH_4 (Figs. 5, 6). When $\delta^{2}H_{CH_4}$ and $\delta^{13}C_{CH_4}$ values were plotted against each other, many samples clustered tightly near the signature of atmospheric CH_4 (Fig. 7). Some points, like those from caves 25 and 26, plotted near the expected trend of partial atmospheric CH_4 oxidation by methanotrophy. The modeled $\delta^{13}C_{CH_4}$ and $\delta^{2}H_{CH_4}$ values of cave air overlapped with our collected samples (Figs. 5, 6, 7, Supplemental Table 3).

4. Discussion

4.1. Subsurface-Surface Atmospheric Exchange

The concentrations and stable isotopic compositions of CH_4, CO_2, and Rn in cave air overlapped and diverged from those of the atmosphere. This suggests that atmospheric and internal cave processes influenced the composition of cave air. The majority of cave air samples were depleted in CH_4 and enriched in CO_2 relative to the local atmosphere, regardless of the fact that at many study locations local atmospheric CH_4 concentrations were above the globally averaged atmospheric background (1.87 ppmv CH_4; Ciais et al., 2013). This points to processes like *in-situ* CH_4 oxidation and diffusion of air from the epikarst to decrease CH_4 and increase CO_2

Preprints (www.preprints.org) | NOT PEER-REVIEWED | Posted: 29 October 2017 doi:10.20944/preprints201708.0009.v2

concentrations (Fig. 2). Study sites may have had high atmospheric CH_4 concentrations due to their proximity to roads or pastures with local CH_4 sources (Gioli et al., 2012; Harper et al., 2014).

The decreases in CH_4 concentration in cave air were correlated with increases in the distance from a cave entrance, CO_2 concentration, Rn concentration, and decreases in $\delta^{13}C_{CO_2}$ values (Figs. 2, 3). These parameters tend to be correlated with cave air residence time. The relationship between the distance to a cave entrance and the residence time of air in a particular cave is multivariate and we observed departures from this trend in several caves. Caves 13 and 15 experienced fast airflow, cave air was flowing out of the entrance of cave 26, cave 24 has multiple entrances which likely result in multiple flow paths, in cave 20 the distance scale of the measurements may have been too small to observe a decrease in CH_4 concentration, and internal CH_4 sources, which were present in cave 9, may obscure the relationship.

The concentration of Rn in cave air is known to track cave air residence time and has been observed to correlate with CO_2 concentrations. We observed correlations between cave air CO_2 and Rn concentrations. This matches other observations from the literature (Kowalczk and Froelich, 2010; Gregorič et al., 2011; as well as others). CO_2 concentrations were negatively correlated with CH_4 concentrations. This provides strong evidence that CH_4 concentrations decreased with cave air residence time. Additionally, the $\delta^{13}C_{CO_2}$ values exhibited a continuum between atmospheric values of −10 ‰ at low concentrations and decreased with CO_2 concentrations. The projected $\delta^{13}C_s$ values ranged from −28 to −20 ‰ with an average $\delta^{13}C_{CO_2}$ value of −23.3 ± 0.5 ‰ entering the caves. This matches the $\delta^{13}C_{CO_2}$ of soils of −24 ‰ (Amundson et al., 1998) (Fig. 4). It is possible that the observed source values that are more negative than −24 ‰ may be due to dripwater degassing or fast airflow (Spötl et al., 2005; Garcia-Anton et al., 2014). The $\delta^{13}C_s$ values that are more positive than −24 ‰ may be caused by differential abundances of

Preprints (www.preprints.org) | NOT PEER-REVIEWED | Posted: 29 October 2017 doi:10.20944/preprints201708.0009.v2

C3 and C4 plants above the caves (Breecker et al., 2012). Our CO_2 data show that cave air residence time increased as the CH_4 concentrations and $\delta^{13}C_{CO_2}$ values of cave air decreased, and that the caves in our study are not atypical compared to other caves in the literature.

In some of the caves where we measured Rn concentrations, cave air flow was relatively fast. The average CO_2 and Rn concentrations from these caves were relatively low (cave 33, [CO_2] = 540 ± 20 ppmv, [Rn] = 20 ± 100 Bq m^{-3}; cave 34, [CO_2] = 560 ± 30 ppmv, [Rn] = 200 ± 400 Bq m^{-3}). Despite the similarity to atmospheric CO_2 concentrations in these caves, average CH_4 concentrations were still depleted relative to the atmosphere (cave 33, [CH_4] = 1.07 ± 0.06 ppmv; cave 34, [CH_4] = 1.34 ± 0.06 ppmv). These observations show that an *in-situ* process is removing CH_4 from the cave air because subatmospheric CH_4 concentrations in cave air are still observed in the absence of large increases in CO_2 concentrations as would be expected if CH_4 were only diluted by the arrival of CH_4-free air into caves from soils. These observations agree with other observations of fast CH_4 oxidation in caves (Fernandez-Cortes et al., 2015; Lennon et al., 2017; Warring et al., 2017). Landscape scale CH_4 flux data from karst areas are needed to estimate the size of the karst sink.

4.2. Sources and Stable Isotopic Composition of Methane

Our CH_4 concentration $\delta^{13}C_{CH_4}$ and $\delta^{2}H_{CH_4}$ data from caves show that caves have sources of non-atmospheric CH_4. Additional sources of CH_4 entering caves were detected by CH_4 concentrations above the atmospheric background in three caves, namely (i) cave 3, Indiana, (ii) cave 22, Tennessee, and (iii) cave 32, New Zealand. Caves with CH_4 concentrations above the

Preprints (www.preprints.org) | NOT PEER-REVIEWED | Posted: 29 October 2017 doi:10.20944/preprints201708.0009.v2

atmospheric background appear to be uncommon, and understanding if there is a systematic change in karst landscapes from smaller order to higher order drainages awaits future work.

The values of $\delta^{13}C_{CH_4}$ and $\delta^{2}H_{CH_4}$ show that non-atmospheric CH_4 enters several caves because they were more negative than those predicted by the oxidation of atmospheric CH_4 *via* methanotrophy or reaction with ·OH. Other studies have also shown microbially produced CH_4 entering caves (Mattey et al., 2013; Webster et al., 2016). Our data point to the methanogenic sources of acetate fermentation and carbonate reduction (Fig. 7). Mixing between residual atmospheric CH_4 after partial methanotophic oxidation and CH_4 from acetate fermentation in the soil-epikarst-cave system will generally cause a decrease in the $\delta^{13}C_{CH_4}$ and $\delta^{2}H_{CH_4}$ values of cave air compared to the atmospheric oxidation, and this is supported by our modeling (Figs. 5, 6). Caves 23, 24, and 26 all appear to be influenced by acetoclastic methanogenesis.

CH_4 produced from carbonate reduction is inferred to enter the caves based on samples that had $\delta^{2}H_{CH_4}$ values that were roughly equal to, or more positive than atmospheric values (Fig. 7). The stable isotopic compositions of CH_4 from caves 5, 15, 25, and 27 can be explained by partial methanotrophic consumption of CH_4 generated from carbonate reduction with the strongest source signal in cave 5 (Fig. 7). CO_2 reduction is typically observed in lake sediments, but has been observed in oxidizing environments such as biological soil crusts in deserts after rain events (Angel et al., 2011). We hypothesize that karst environments, which are less oxidizing, exhibit similar behavior. Our data show that carbonate reduction and acetate fermentation can occur in similar environments over large spatial scales and are not limited to aquatic and arctic environments.

Sites of methanogenesis in or near the studied cave systems may include waterlogged soils above caves, cave soils themselves, and the epikarst. It is possible that after rain events anoxic

Preprints (www.preprints.org) | NOT PEER-REVIEWED | Posted: 29 October 2017 doi:10.20944/preprints201708.0009.v2

micro niches occur in soil, the epikarst, or caves themselves and that the generated CH_4 is dissolved and later introduced into caves with drip waters. We confirmed that dissolved CH_4 outgasses in drip water of cave 32, which was situated underneath a wetland, by placing our CH_4 detecting probe near the water and measuring increased CH_4 concentrations in its vicinity. We confirmed that *in-situ* CH_4 production can take place in locally anoxic environments within caves by measuring CH_4 concentrations close to a bat guano deposit in cave 25, Tennessee (site 4h; average CH_4 concentration = 0.3 ± 0.5 ppmv). Time series measurements near the large bat guano deposit showed that CH_4 concentrations oscillated between 0.5 ppmv and 0.1 ppmv over the course of seconds, presumably in response to episodic migration of CH_4 bubbles through the moist guano (similar oscillations in ammonia, NH_3, were also observed). Additionally, we observed circumstantial evidence for local *in-situ* CH_4 production in cave 3 because measured CH_4 concentrations upstream of a restroom in the cave were low, while measured CH_4 concentrations downstream of the restroom were enhanced. Our data show that caves are capable of expressing elevated CH_4 concentrations due to *in-situ* CH_4 production when accumulations of organic matter, such as guano or plant material, foster methanogenesis or when dissolved CH_4 from waters outgasses into cave air.

We observed minor amounts of thermogenic CH_4 entering in at least one cave. Locally elevated CH_4 concentrations in cave 9 (Mammoth Cave, Kentucky) were associated with a known hydrocarbon seep that is also transporting sulfide (Olson, 2013). Elevated CH_4 concentrations, thought to derive from thermogenic CH_4, have also been observed at sulfidic springs in *Cueva de Villa Luz* (Webster et al., 2017). Some $\delta^{13}C_{CH_4}$ and $\delta^{2}H_{CH_4}$ values in cave air, i.e. two of the samples from cave 24, are compatible with thermogenic CH_4 isotopic signatures (e.g., Schoell, 1988; Etiope et al., 2009; Fig. 7). It cannot be excluded that small fluxes of CH_4 from shales or

Preprints (www.preprints.org) | NOT PEER-REVIEWED | Posted: 29 October 2017 doi:10.20944/preprints201708.0009.v2

hydrocarbon deposits underlying the limestone are entering caves through natural fractures, but our present isotope data cannot confirm this source for cave 24. The Antes and Utica shales, which contain hydrocarbon gases, are stratigraphically below cave 24 (Coleman et al., 2014), and geologic faults and joints, which are often aligned with caves, may serve as conduits for the flow of hydrocarbons (Powell, 1969). A confirmation of hydrocarbons entering from deep sources may be obtained through measurements of 'radiocarbon-dead' CO_2, Rn, and ethane.

4.3. Methane Oxidation Mechanisms

The combination of $\delta^{13}C_{CH_4}$ and $\delta^{2}H_{CH_4}$ values allow for inferences to be made about how CH_4 oxidizing reactions in karst environments. We distinguish between two scenarios with distinct sets of assumptions. Many isotopic compositions of CH_4 in this study cannot be accounted for in the first scenario in which we assume that (i) CH_4 enters the caves from the atmosphere, through acetate fermentation, and through carbonate reduction, and that (ii) CH_4 is removed from cave air through reactions involving the ·OH. Conversely, in a second scenario, if it is assumed that (i) sources of CH_4 in cave air include the atmosphere, acetate fermentation, and carbonate reduction, and that (ii) CH_4 is removed from cave air by methanotrophy, all of the points fall within the plausibility envelope of the model, suggesting that methanotrophy is the mechanism responsible for removing CH_4 from cave air (Fig. 7). Consideration of an additional source of thermogenic CH_4 (natural gas) from deep geologic sources enlarges the plausibility fields of both prior scenarios to encompass all of the data. Furthermore, the modeled isotopic composition of cave air, which has the same assumptions as the second scenario, overlays comparably with our data set.

Preprints (www.preprints.org) | NOT PEER-REVIEWED | Posted: 29 October 2017 doi:10.20944/preprints201708.0009.v2

Our $\delta^{13}C_{CH_4}$ and $\delta^{2}H_{CH_4}$ data also agree with observations of $\delta^{13}C_{CH_4}$ and $\delta^{2}H_{CH_4}$ from a cave in Indiana where it appeared that CH_4 from both acetate fermentation and carbonate reduction influenced cave air geochemistry (Webster et al., 2016). Additionally, our data resemble an arctic system characterized by acetoclastic and hydrogenotrophic CH_4 sources and methanotrophy (McCalley et al., 2014). Our isotopic evidence for *in-situ* microbial CH_4 oxidation in caves is corroborated by recent results from *in-situ* mesocosm experiments in Vietnam where cave rocks with live microorganisms were shown to consume CH_4 even in cases where surface soils were very thin to non-existent (Lennon et al., 2017; Nguyễn-Thuỳ et al., 2017; Waring et al., 2017).

5. Conclusions

1) CH_4 consumption is the dominant process in karst landscapes. Subterranean karst air generally shows subatmospheric CH_4 concentrations. CH_4 and CO_2 concentrations were negatively correlated in cave air showing that as the residence time of cave air increases the CH_4 concentration of cave air decreases. This shows that an *in-situ* process is responsible for the removal of CH_4 from cave air.

2) The stable isotopic composition of CH_4 in studied caves suggests that CH_4 is being oxidized by microbial methanotrophy. This evidence adds to reports that methanotrophy is the mechanism by which CH_4 is rapidly removed in cave air (Mattey et al., 2013; McDonough et al., 2016; Webster et al., 2016; Lennon et al., 2017, Waring et al., 2017). The observations of sub-atmospheric CH_4 concentrations in cave air from this and other studies show that karst is behaving as a global CH_4 sink.

 doi:10.20944/preprints201708.0009.v2

392 3) The stable isotopic composition of CH_4 in the studied caves suggests that, in addition to
393 atmospheric CH_4, at least two additional CH_4 sources are present in some caves. We
394 suggest that the sources include CH_4 produced from acetate fermentation and from CO_2
395 reduction. These data corroborate recent findings of partially oxidized CH_4 entering cave
396 air from acetate fermentation and CO_2 reduction in Indiana (Webster et al., 2016). These
397 observations of CH_4 production by acetate fermentation and carbonate reduction suggest
398 that both processes happen over a wide scale in the environment.

399

400 **Acknowledgements**

401 This material is based upon work supported by the U.S. Department of Energy, Office of
402 Science, Office of Basic Energy Sciences, Chemical Sciences, Geosciences, and Biosciences
403 Division under Award Number DE-SC0006978. This study was partially funded by NASA ASTEP
404 (Award # NNX11AJ01G) and a National Speleological Society research grant. We thank J.
405 Forsythe of Lost River Cave (cave 7) and R. S. Toomey III of Mammoth Cave National Park for
406 granting access. Members of the Bloomington Indiana Grotto facilitated access to caves in Indiana.
407 The Richard Blenz Nature Conservancy permitted access to cave 35. We thank M. Lefticariu and
408 J. Hayden-Moore of Little Egypt Grotto in Carbondale, Illinois for providing assistance and access
409 to gas sampling in cave 36 (SE Missouri). T.V. Royer in SPEA at Indiana University made
410 analytical gas chromatography available. We are grateful for constructive comments from
411 anonymous reviewers.

412

413

References

Amundson, R., Stern, L., Baisden, T., Wang, Y., 1998. The isotopic composition of soil and soil-respired CO_2. Geoderma 82, 83–114. http://dx.doi.org/10.1016/S0016-7061(97)00098-0

Angel, R., Matthies D., Conrad, R., 2011. Activation of methanogenesis in arid biological soil crusts despite the presence of oxygen. PLoS ONE 6(5), e20453. http://dx.doi.org/10.1371/journal.pone.0020453

Batiot-Guilhe, C., Seidel, J.-L., Jourde, H., Hébrard, O., Bailly-Comte, V., 2007. Seasonal variations of CO_2 and ^{222}Rn in a Mediterranean sinkhole – sping (Causse d'Aumelas, SE France). International Journal of Speleology 36(1), 51-56.

Breecker, D.O., Payne, A.E., Quade, J., Banner, J.L., Ball, C.E., Meyer, K.W., Cowan, B.D., 2012. The sources and sinks of CO_2 in caves under mixed woodland and grassland vegetation. Geochimica et Cosmochimica Acta 96, 230-246. http://dx.doi.org/10.1016/j.gca.2012.08.023

Ciais, P., Sabine, C., Bala, G., Bopp, L., Brovkin, V., Canadell, J., Chhabra, A., DeFries, R., Galloway, J., Heimann, M., Jones, C., Le Quéré, C., Myneni, R.B., Piao, S., Thornton, P., 2013. Carbon and other biogeochemical cycles. *In* (Stocker, T.F., Qin, D., Plattner, G.-K., Tignor, M., Allen, S.K., Boschung, A., Nauels, A., Xia, Y., Bex, V., Midgley, P.M., eds.) Climate Change 2013: The Physical Science Basis. Contribution to Working Group I to the Fifth Assessment Report of the Intergovernmental Panel on Climate Change. Cambridge University Press, Cambridge, United Kingdom and New York, NY, USA.

434 Coleman D.D., Risatti J.B., Schoell M., 1981. Fractionation of carbon and hydrogen isotopes by
435 methane-oxidizing bacteria. Geochimica et Cosmochimica Acta 45(7), 1033-1037.
436 http://dx.doi.org/10.1016/0016-7037(81)90129-0

437 Coleman, J.L., Jr., Ryder, R.T., Milici, R.C., Brown, S., 2014. Overview of the potential and
438 identified petroleum source rocks of the Appalachian Basin, Eastern United States. *In*
439 (Ruppert, L.F., Ryder, R.T., eds.) Coal and Petroleum Resources in the Appalachian
440 basin; Distribution, Geologic Framework, and Geochemical Character: U.S. Geological
441 Survey Professional Paper 1708, http://dx.doi.org/10.3133/pp1708G.13

442 Cunningham, K.I., LaRock, E.J., 1991. Recognition of microclimate zones through radon
443 mapping, Lecheguilla Cave, Carlsbad Caverns National Park, New Mexico. Health
444 Physics 61(4), 493-500.

445 Dlugokencky, E.J., Houweling, S., Bruhwiler, L., Masarie, K.A., Lang, P.M., Miller, J.B., Tans,
446 P.P., 2003. Atmospheric methane levels off: Temporary pause or a new steady state?
447 Geophysical Research Letters 30 (1992), http://dx.doi.org/10.1029/2003GL018126

448 Dlugokencky, E.J., Nisbet, E.G., Fisher, R., Lowry, D., 2011. Global atmospheric methane:
449 budget changes, and dangers. Phil. Trans. R. Soc. A 369, 2058-2072.
450 http://dx.doi.org/10.1098/rsta.2010.0341

451 Etiope G., Feyzullayev A., Baciu C.L., 2009. Terrestrial methane seeps and mud volcanoes: a
452 global perspective of gas origin. Marine and Petroleum Geology 26, 333-344.
453 http://dx.doi.org/10.1016/j.marpetgeo.2008.03.001

454 Feisthauer, S., Vogt, C., Modrzynski, J., Szlenkier, M., Krüger, M., Siegert, M., Richnow, H.-H.,
455 2011. Different types of methane monooxygenases produce similar carbon and hydrogen

 doi:10.20944/preprints201708.0009.v2

456 isotope fraction patterns during methane oxidation. Geochimica et Cosmochimica Acta
457 75(5), 1173-1184. http://dx.doi.org/10.1016/j.gca.2010.12.006

458 Fernandez-Cortes, A., Cuezva, S., Alvarez-Gallego, M., Garcia-Anton, E., Pla C., Benavente, D.,
459 Jurado V., Saiz-Jimenez, C., Sanchez-Moral, S., 2015. Subterranean atmospheres may act
460 as daily methane sinks. Nature Communications 6(7003).
461 http://dx.doi.org/10.1038/ncomms8003

462 Garcia-Anton, E., Cuezva, S., Fernandez-Cortes, A., Benavente, D., Sanchez-Moral, S., 2014.
463 Main drivers of diffusive and advective processes of CO_2-gas exchange between a
464 shallow vadose zone and the atmosphere. International Journal of Greenhouse Gas
465 Control 21, 113-129. http://dx.doi.org/10.1016/j.ijggc.2013.12.006

466 Ford, D., Williams, P., 2007. Karst Hydrogeology and Geomorphology. John Wiley & Sons Ltd,
467 England.

468 Gioli, B., Toscano, P., Lugato, E., Matese, A., Migilietta, F., Zaldei, A., Vaccari, F.P., 2012.
469 Methane and carbon dioxide fluxes and source partitioning in urban areas: The case study
470 of Florence, Italy. Environmental Pollution 164, 125-131.
471 http://dx.doi.org/10.1016/j.envpol.2012.01.019

472 Gregorič, A., Zidanšek, A., Vaupotič, J., 2011. Dependence of radon levels in Postojna Cave on
473 outside air temperature. Natural Hazards and Earth System Sciences 11, 1523-1528.
474 http://dx.doi.org/ 10.5194/nhess-11-1523-2011

475 Gregorič, A., Vaupotič, J., Šebela, S., 2014. The role of cave ventilation in governing cave air
476 temperature and radon levels (Postojna Cave, Slovenia). International Journal of
477 Climatology 34(5), 1488-1500. http://dx.doi.org/10.1002/joc.3778

478 Harper, L.A., Weaver, K.H., De Visscher, A., 2014. Dinitrogen and methane gas production
479 during the anaerobic/anoxic decomposition of animal manure. Nutrient Cycling in
480 Agroecosystems 100(1), 53-64. http://dx.doi.org/10.1007/s10705-014-9626-9

481 Hutchens, E., Radajewski, S., Dumont, M.G., McDonald, I.R., Murrell, J.C., 2004. Analysis of
482 methanotrophic bacteria in Movile Cave by stable isotope probing. Environmental
483 Microbiology 6(2), 111-120. http://dx.doi.org/10.1046/j.1462-2920.2003.00543.x

484 Jones, D.S., Albrecht, H.L., Dawson, K.S., Schaperdoth, I., Freeman, K.H., Pi, Y., Pearson, A.,
485 Macalady, J.L., 2012. Community genomic analysis of an extremely acidophilic sulfur
486 oxidizing biofilm. The ISME Journal 6, 158-170. http://dx.doi.org/10.1038/ismej.2011.75

487 Kirschke, S., Bousquet, P., Ciais, P., Saunois, M., Canadell, J.G., Dlugokencky, E.J.,
488 Bergamaschi, P., Bergmann, D., Blake, D.R., Bruhwiler, L., Cameron-Smith, P.,
489 Castaldi, S., Chevallier, F., Feng, L., Fraser, A., Heimann, M., Hodson, E.L., Houweling,
490 S., Josse, B., Fraser, P.J., Krummel, P.B., Lamarque, J.-F., Langenfelds, R.L., Le Quéré,
491 C., Naik, V., O'Doherty, S., Palmer, P.I., Pison, I., Plummer, D., Poulter, B., Prinn, R.G.,
492 Rigby, M., Ringeval, B., Santini, M., Schmidt, M., Schindell, D.T., Simpson, I.J., Spahni,
493 R., Steele, L.P., Strode, S.A., Sudo, K., Szopa, S., van der Werf, G.R., Voulgarakis, A.,
494 van Weele, M., Weiss, R.F., Williams, J.E., Zeng, G., 2014. Three decades of global
495 methane sources and sinks. Nature Geoscience 6, 812-8123.

496 Keeling, R.F., Piper, S.C., Bollenbacher, A.F., Walker, S.J., 2010. Monthly atmospheric $^{13}C/^{12}C$
497 isotopic ratios for 11 SIO stations. *In* Trends: A Compendium of Data on Global Change.
498 Carbon Dioxide Information Analysis Center, Oak Ridge National Laboratory, U.S.
499 Department of Energy, Oak Ridge, Tenn., U.S.A.

500 Kowalczk, A.J., Froelich, P.N., 2010. Cave air ventilation and CO_2 outgassing by radon-222
501 monitoring: How fast do caves breathe? Earth and Planetary Science Letters 289, 209-
502 219. http://dx.doi.org/10.1016/j.epsl.2009.11.010

503 Lennon, J.T., Nguyễn-Thùy, D., Phạm, T.M., Drobniak, A., Tạ, P.H., Phạm, N.Đ., Streil, T.,
504 Webster, K.D., Schimmelmann, A., 2017. Microbial contributions to subterranean
505 methane sinks. Geobiology 15(2), 254-258. http://dx.doi.org/10.1111/gbi.12214

506 Mattey, D.P., Fairchild, I.J., Atkinson, T.C., Latin, J.-P., Ainsworth, M., Durell, R., 2010.
507 Seasonal microclimate control of calcite fabrics, stable isotopes and trace elements in
508 modern speleothem from St. Michaels Cave, Gibraltar. *In* (Pedley, H.M., Rogerson, M.
509 eds.) Tufas and Speleothems: Unravelling the Microbial and Physical Controls:
510 Geological Society, London, Special Publications 336, 323-344.
511 http://dx.doi.org/10.1144/SP336.17

512 Mattey, D.P., Fisher, R., Atkinson, T.C., Latin, J.-P., Durrell, R., Ainsworth, M., Lowry, D.,
513 Fairchild, I.J., 2013. Methane in underground air in Gibraltar karst. Earth and Planetary
514 Science Letters 374, 71-80. http://dx.doi.org/10.1016/j.epsl.2013.05.011

515 McCalley, C.K., Woodcroft, B.J., Hodgkins, S.B., Wehr, R.A., Kim, E.-H., Mondav, R., Crill,
516 P.M., Chanton, J.P., Rich, V.I., Tyson, G.W., Saleska, S.R., 2014. Methane dynamics
517 regulated by microbial community response to permafrost thaw. Nature 514, 478-481.
518 http://dx.doi.org/10.1038/nature13798

519 McDonough, L.K., Iverach, C.P., Beckman, S., Manfield, M., Rau, G.C., Baker, A., Kelly,
520 B.F.J., 2016. Spatial variability of cave-air carbon dioxide and methane concentrations

and isotopic compositions in a semi-arid karst environment. Environmental Earth Sciences 75(700), http://dx.doi.org/10.1007/s12665-016-5497-5

Miller, J.B., Mack, K.A., Dissly, R., White, J.W.C., Dlugokencky, E.J., Tans, P.P., 2002. Development of analytical methods and measurements of $^{13}C/^{12}C$ in atmospheric CH_4 from the NOAA Climate Monitoring and Diagnostics Laboratory Global Air Sampling Network. Journal of Geophysical Research: Atmospheres 107(D13), ACH 11-1-ACH 11-15. http://dx.doi.org/10.1029/2001JD000630

Nisbet, E.G., Dlugokencky, E.J., Manning, M.R., Lowry, D., Fisher, R.E., France, J.L., Michel, M.E., Miller, J.B., White, W.J.C., Vaughn, B., Bousquet, P., Pyle, J.A., Warwick, N.J., Cain, M., Brownlow, R., Zazzeri, G., Lanoisellé, M., Manning, A.C., Gloor, E., Worthy, D.E.J., Brunke, E.-G., Labuschagne, C., Wolff, E.W., Ganesan, A.L., 2016. Rising atmospheric methane: 2007-2014 growth and isotopic shift. Global Biogeochemical Cycles 30, 1356-1370. http:///dx.doi.org/10.1002/2016GB005406

Nguyễn-Thuỳ, D., Schimmelmann, A., Nguyễn-Văn, H., Drobniak, A., Lennon, J.T., Tạ, P.H., Nguyễn, N.T.Á., (2017). Subterranean microbial oxidation of atmospheric methane in cavernous tropical karst. *Chemical Geology*. https://doi.org/10.1016/j.chemgeo.2017.06.014

Olson, R., 2013. Potential effects of hydrogen sulfide and hydrocarbon seeps on Mammoth Cave ecosystems. Mammoth Cave Research Symposia. Paper 28. http://digitalcommons.wku.edu/mc_reserch_symp/10th_Research_Symposium_2013/Research_Posters/28

Palmer, A.N., 1991. Origin and morphology of limestone caves. Geological Society of America

543 Bulletin 103(1), 1-21. http://dx.doi.org/10.1130/0016-
544 7606(1991)103<0001:OAMOLC>2.3.CO;2

545 Peyraube, N., Lastennet, R., Denis, A., Malaurent, P., 2013. Estimation of epikarst air P_{CO_2} using
546 measurements of water $\delta^{13}C_{TDIC,}$ cave air P_{CO_2} and $\delta^{13}C_{CO_2}$. Geochimica et
547 Cosmochimica Acta 118, 1-17. http://dx.doi.org/10.1016/j.gca.2013.03.046

548 Peyraube, N., Lastennet, R., Villanueva, J.D., Houillon, N., Malaurent, P., Denis, A., 2016.
549 Effect of diurnal and seasonal temperature variation on Cussac cave ventilation using
550 CO_2 assessment. Theoretical and Applied Climatology, http://dx.doi.org/10.1007/s00704-
551 016-1824-8

552 Powell, R.L. 1969. Base level, and climatic controls of karst groundwater zones in South-Central
553 Indiana. Indiana Academy of Science, 281-291.

554 Sarbu, S.M., Kane, T.C., Kinkle, B.K., 1996. A chemoautotrophically based cave ecosystem.
555 Science 272(5270), 1953-1955. http://dx.doi.org/10.1126/science.272.5270.1953

556 Saueressig, G., Crowley, J.N., Bergamaschi, P., Brühl, C., Brennikmeijer, C.A.M., Fischer, H.,
557 2001. Carbon 13 and D kinetic isotope effects in the reactions of CH4 with $O(^1D)$ and
558 OH: New laboratory measurements and their implications for the isotopic composition of
559 stratospheric methane. Journal of Geophysical Research 106 (D19), 23127–23138.
560 http://dx.doi.org/10.1029/2000JD000120

561 Schoell, M., 1988. Multiple origins of methane in the Earth, *in* Schoell, M. ed. Origins of
562 Methane in the Earth. Chemical Geology 71, 1-10. http://dx.doi.org/10.1016/0009-
563 2541(88)90101-5

564 Spötl, C., Fairchild, I.J., Tooth, A.F., 2005. Cave air control on dripwater geochemistry, Obir
565 Caves (Austria): Implications for speleothem deposition in dynamically ventilated caves.
566 Geochimica et Cosmochimica Acta 69(10), 2451-2468.
567 http://dx.doi.org/10.1016/j.gca.2004.12.009

568 Sussman, R., Forster, F., Rettinger, M., Bousquet, P., 2012. Renewed methane increase for five
569 years (2007-2011) observed by solar FTIR spectrometry. Atmospheric Chemistry and
570 Physics 12, 4885-4891. http://dx.doi.org/10.5194/acp-12-4885-2012

571 Templeton, A., Chu, K.-H., Alvarez-Cohen, L., Conrad, M.E., 2006. Variable carbon isotope
572 fractionation expressed by aerobic CH_4-oxidizing bacteria. Geochimica et Cosmochimica
573 Acta 70(7), 1739-1752. http://dx.doi.org/10.1016/j.gca.2005.12.002

574 Townsend-Small, A., Tyler, S.C., Pataki, D.E., Xu, X., Christensen, L.E., 2012. Isotopic
575 measurements of atmospheric methane in Los Angeles, California, USA: Influence of
576 "fugitive" fossil fuel emissions. Journal of Geophysical Research 117(D07308).
577 http://dx.doi.org/10.1029/2011JD016826

578 Tu, K.P., Brooks, P.D., Dawson, T.E., 2001. Using septum-capped vials with continuous-flow
579 isotope ratio mass spectrometric analysis of atmospheric CO_2 for Keeling plot
580 applications. Rapid Communications in Mass Spectrometry 15(12), 952-956.
581 http://dx.doi.org/10.1002/rcm.320

582 Waring, C.L., Hankin, S.L., Griffith, D.W.T., Kertesz, M.A., Kobylski, V., Wilson, N.L.,
583 Coleman, N.V., Kettlewell, G., Zlot, R., Bosse, M., Bell, G., 2017. Scientific Reports
584 7(8314). http://dx.doi.org/10.1038/s41598-017-07769-6

585 Weary, D.J., Doctor, D.H., 2014. Karst in the United States: A digital map compilation and
586 database: U.S. Geological Survey Open-File Report 2014–1156.
587 http://dx.doi.org/10.3133/ofr20141156

588 Webster, K.D., Mirza, A., Deli, J.M., Sauer, P.E., Schimmelmann, A., 2016. Consumption of
589 atmospheric methane in a limestone cave in Indiana, USA. Chemical Geology 443, 1-9.
590 http://dx.doi.org/10.1016/j.chemgeo.2016.09.020

591 Webster, K.D., Rosales Lagarde, L., Sauer, P.E., Schimmelmann, A., Lennon, J.T., Boston, P.J.,
592 2017. Isotopic evidence for the migration of thermogenic methane into a sulfidic cave,
593 Cueva de Villa Luz, Tabasco, Mexico. Journal of Cave and Karst Studies 79(1), 24-34.
594 https://caves.org/pub/journal/PDF/V79/cave-79-01-24.pdf.

595 Whiticar, M.J., 1999. Carbon and hydrogen isotope systematics of bacterial formation and
596 oxidation of methane. Chemical Geology 161, 291-314. http://dx.doi.org/10.1016/S0009-
597 2541(99)00092-3

598

Preprints (www.preprints.org) | NOT PEER-REVIEWED | Posted: 29 October 2017 doi:10.20944/preprints201708.0009.v2

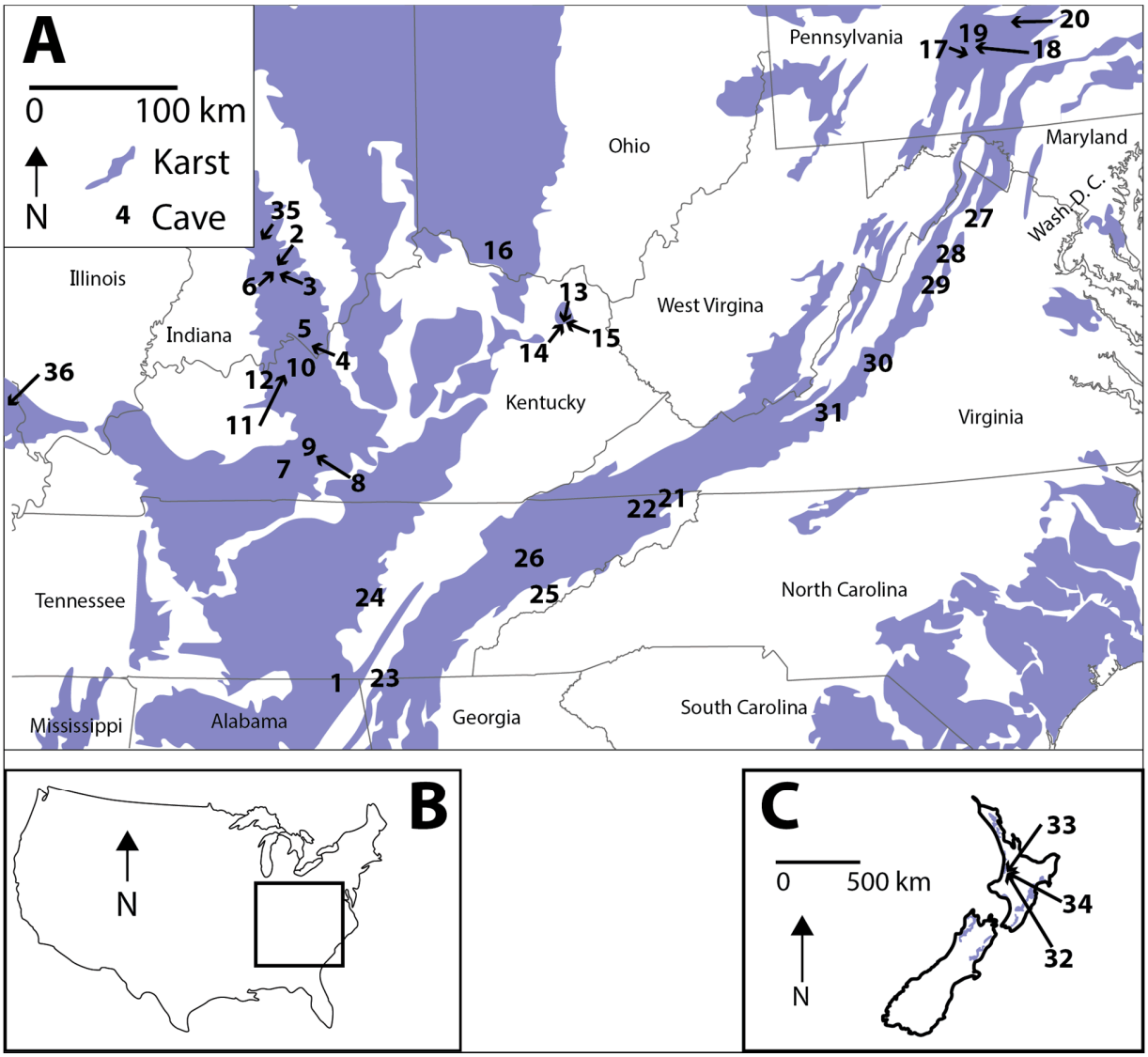

599

600 **Figure 1.** Locations of the U.S. study caves in their regional context (A) and within the contiguous
601 USA (B). The location of the New Zealand caves are presented in C. Karst land cover data were
602 obtained from Weary and Doctor (2014) and Ford and Williams (2007).

603

Preprints (www.preprints.org) | NOT PEER-REVIEWED | Posted: 29 October 2017 doi:10.20944/preprints201708.0009.v2

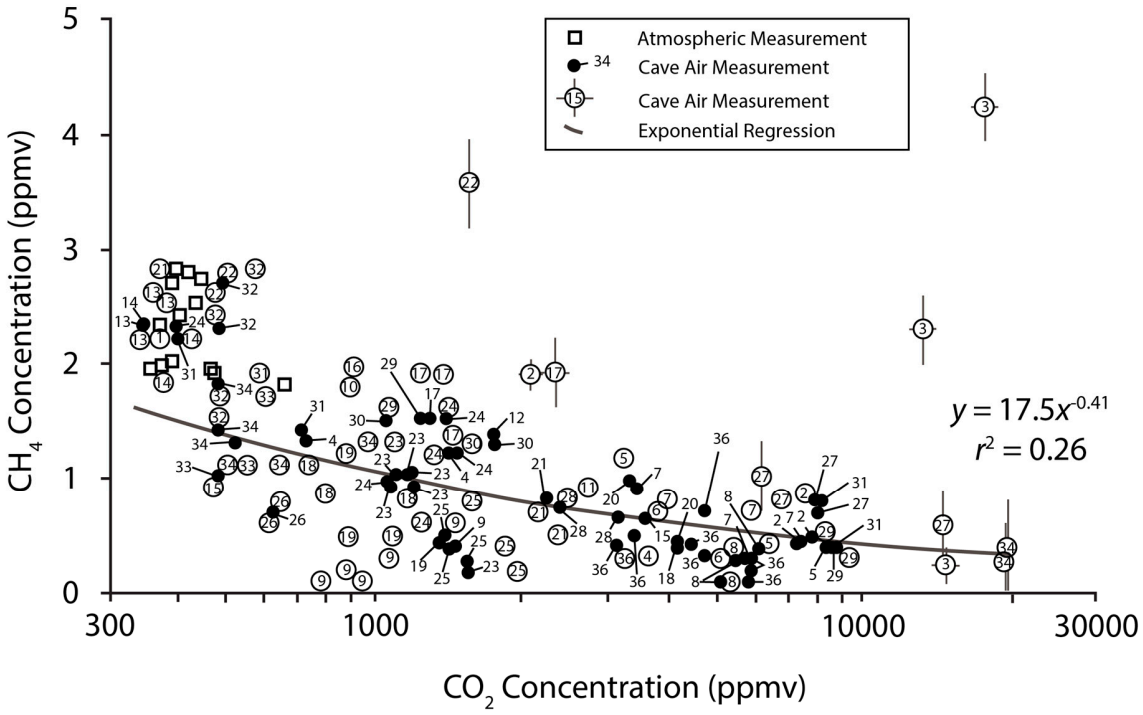

604

605 **Figure 2.** CH_4 concentrations *versus* CO_2 concentrations in studied caves. The majority of samples
606 appear to follow an inverse power law relationship with CH_4 concentrations being inversely related
607 to CO_2 concentrations (with points from caves 3 and 22 removed from the overall trend). Numbers
608 represent individual caves. For clarity some error bars were omitted from the figure. Data
609 associated with error bars are also representative for typical errors of data where no bars are shown.

610

Preprints (www.preprints.org) | NOT PEER-REVIEWED | Posted: 29 October 2017 doi:10.20944/preprints201708.0009.v2

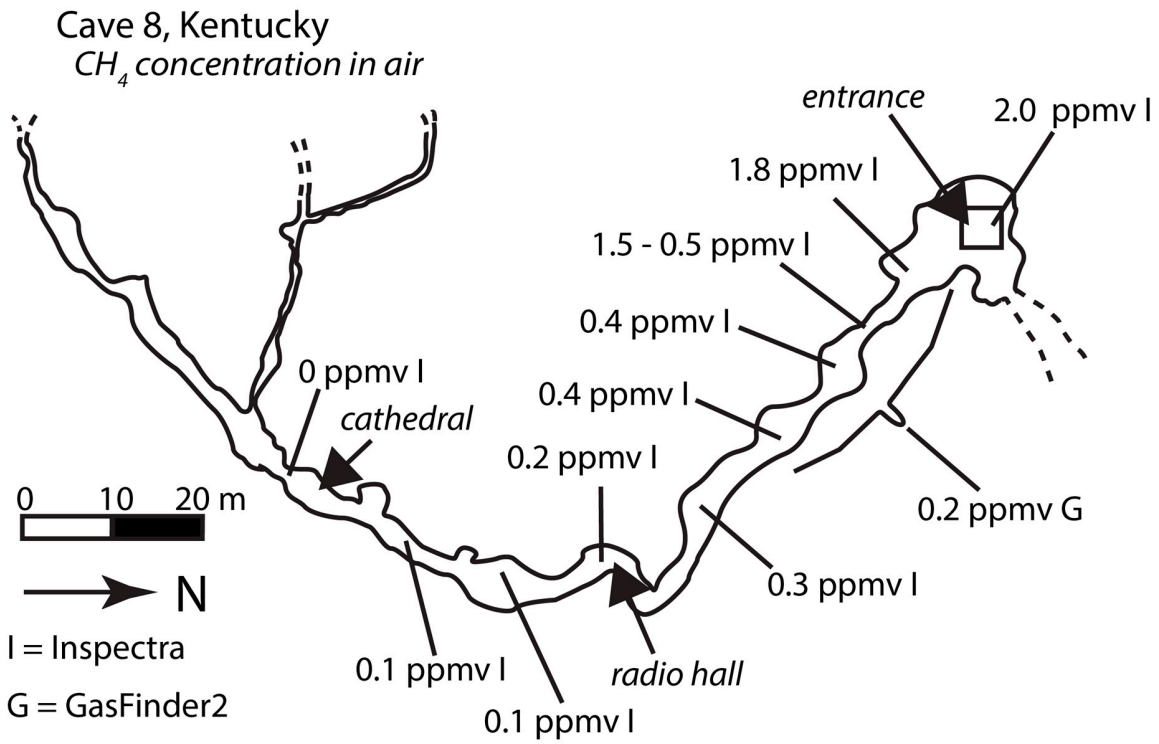

611

612 **Figure 3.** The spatial variation of CH_4 mole faction in the air of cave 8, Kentucky. CH_4
613 concentration dropped sharply from 1.5 to 0.5 ppmv along a narrow path after the first large room,
614 a few tens of meter from the entrance. CH_4 gradually decreased over roughly 100 m down to 0
615 ppmv in the Cathedral room. Both the Inspectra (Gazomat, France assembled by West Systems,
616 Italy) and the GasFinder2 (Boreal Laser Inc., Spruce Grove, Alberta, Canada) use tunable diode
617 lasers.

618

619

620

Preprints (www.preprints.org) | NOT PEER-REVIEWED | Posted: 29 October 2017 doi:10.20944/preprints201708.0009.v2

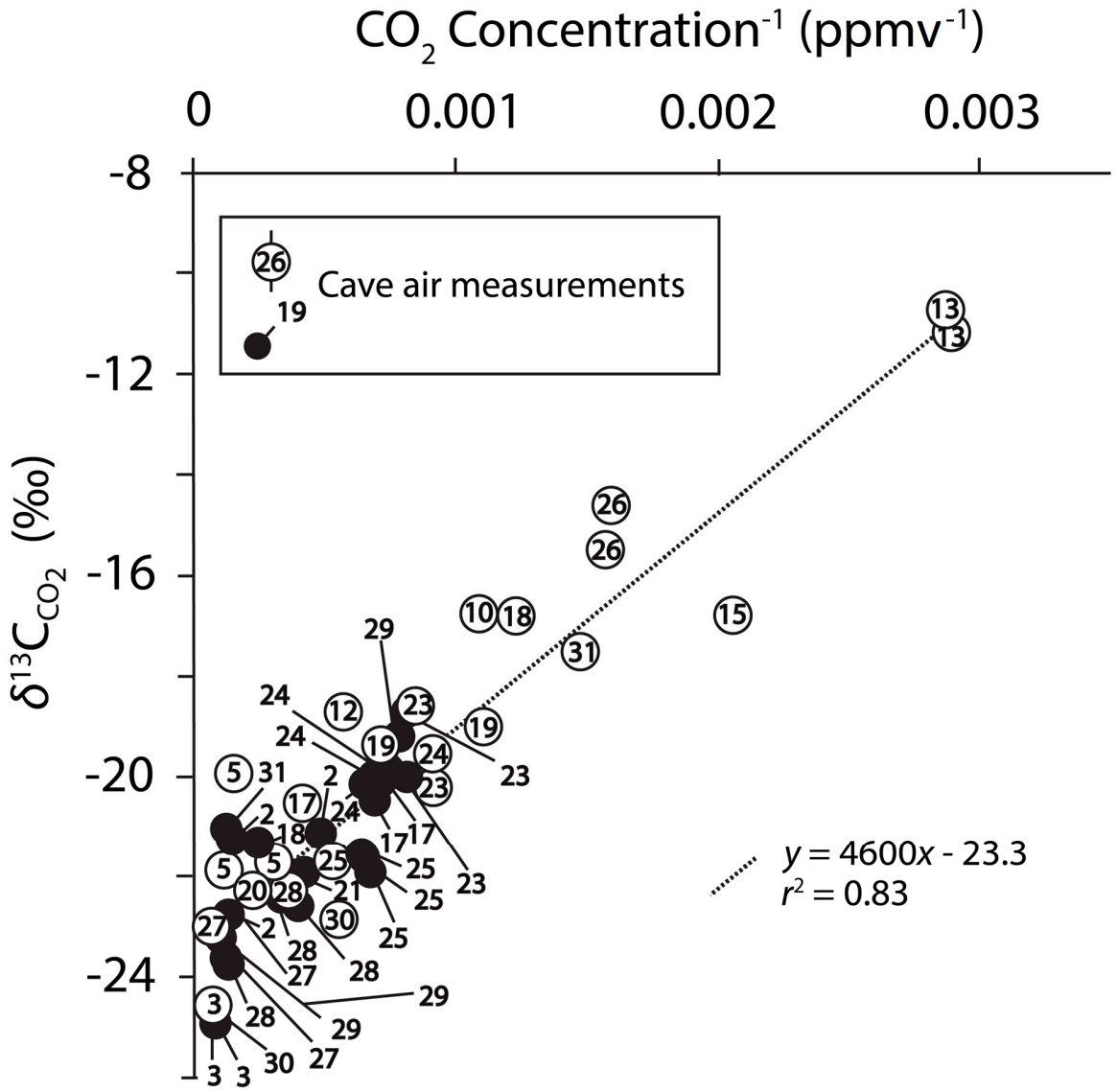

621

622 **Figure 4.** A Keeling plot of $\delta^{13}C_{CO_2}$ *versus* inverse CO_2 concentration in cave air samples. The
623 data show that atmospheric CO_2 is mixing with apparent isotopic endmembers between −33 and
624 −20.4 ‰. A regression analysis of the entire data set shows that the average $\delta^{13}C_{CO_2}$ value entering
625 the caves is −23.3 ± 0.5 ‰. Numbers represent individual caves. Error bars are not included for
626 clarity.

627

Preprints (www.preprints.org) | NOT PEER-REVIEWED | Posted: 29 October 2017 doi:10.20944/preprints201708.0009.v2

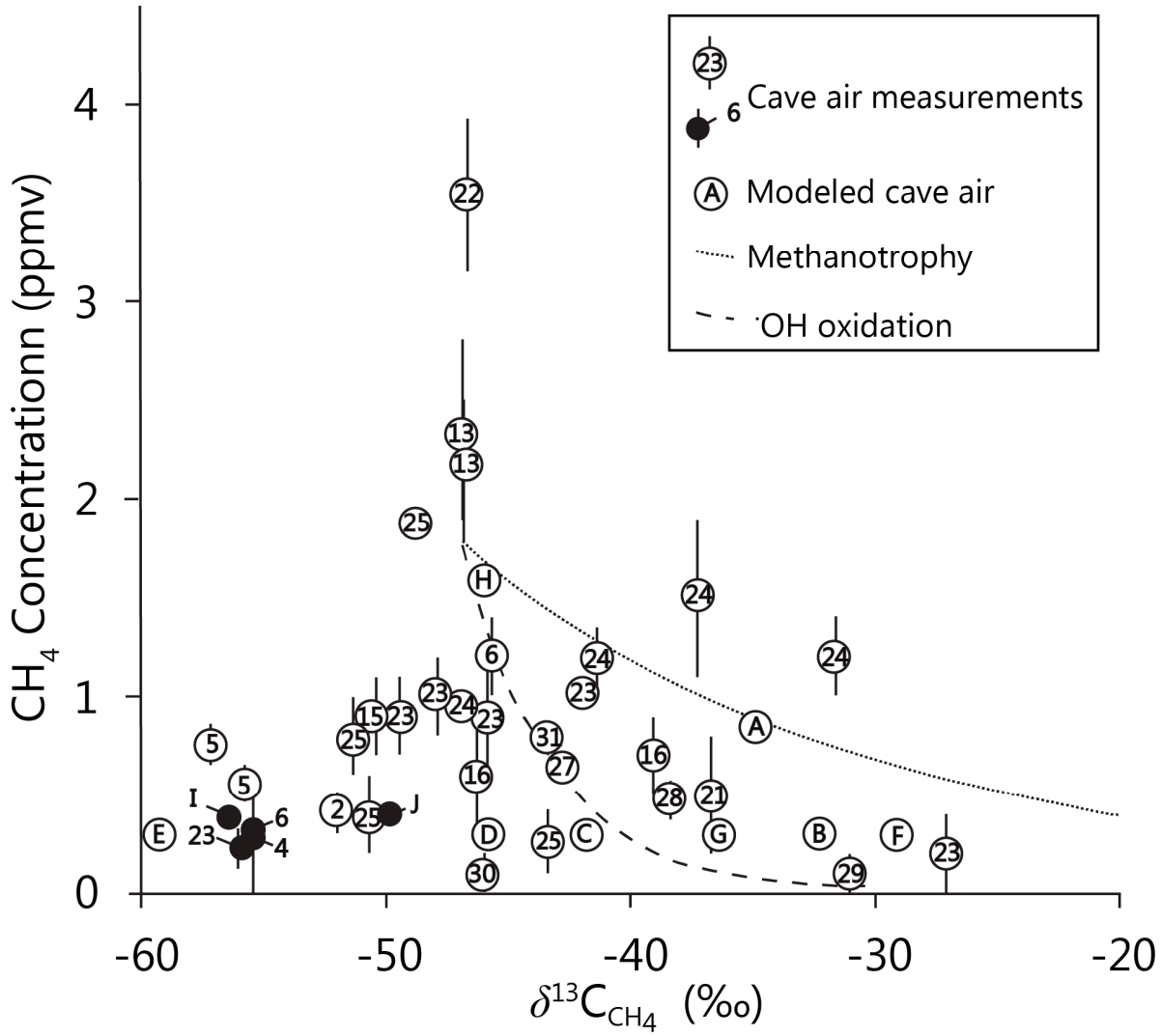

628

629 **Figure 5.** Relationship between CH_4 concentration and $\delta^{13}C_{CH_4}$ in cave air. Some samples plot
630 along the expected relationship between CH_4 concentration and $\delta^{13}C_{CH_4}$ caused either by
631 methanotrophy modeled with an α value of 1.018, or by oxidation with ·OH modeled with an α
632 value of 1.0039. Other samples plot below and to the left of the theoretical shifts of the oxidation
633 trends. Numbers represent individual caves. Note that modeled cave air, represented by letters,
634 also plots left of theoretical methanotrophic oxidation. If error bars are not visible, they are smaller
635 than the data points.

Preprints (www.preprints.org) | NOT PEER-REVIEWED | Posted: 29 October 2017 doi:10.20944/preprints201708.0009.v2

636

637

638

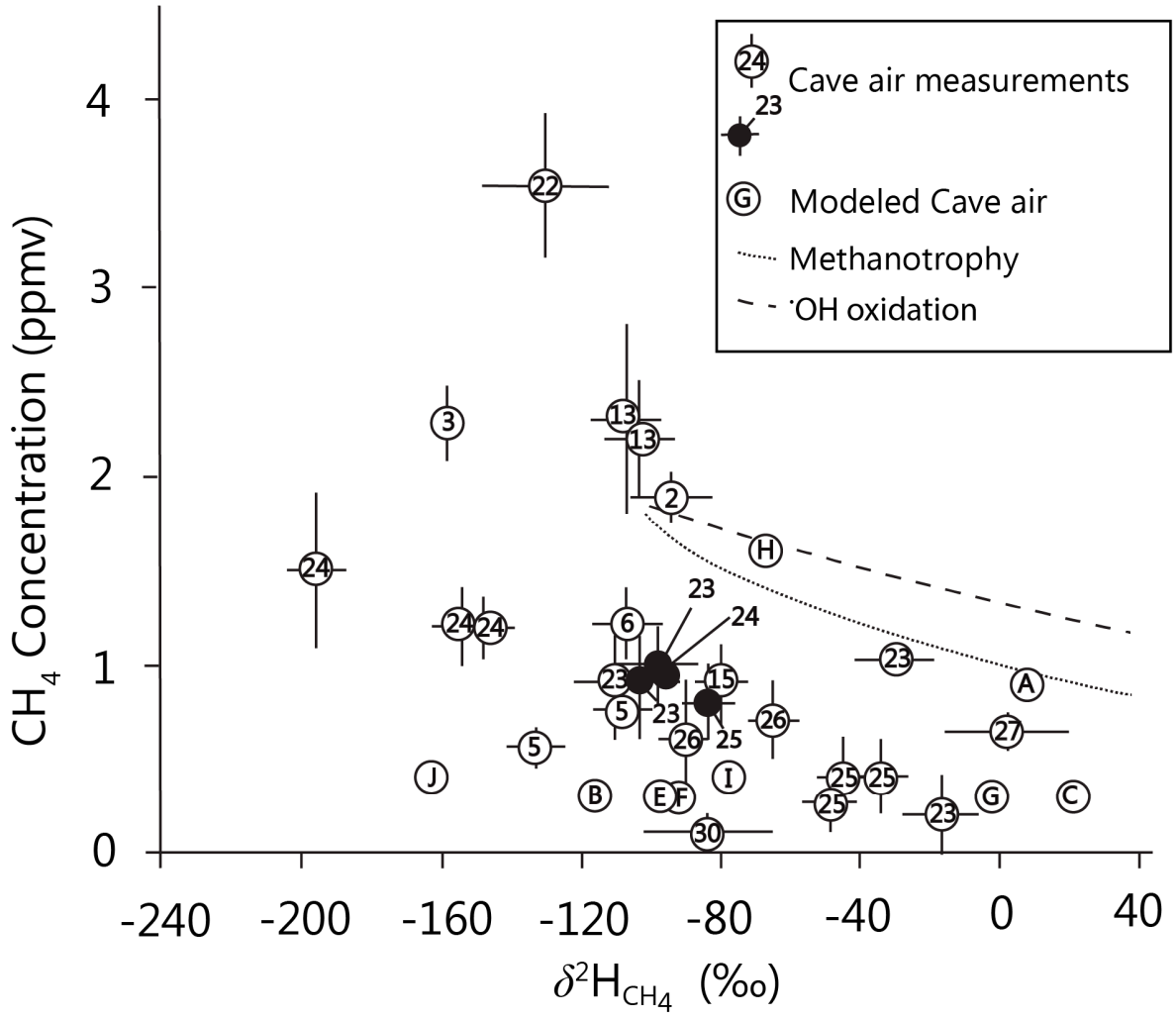

639

640 **Figure 6.** Relationship between methane concentration and $\delta^2H_{CH_4}$ in cave air. Some samples plot

641 along the expected relationship between CH_4 concentration and $\delta^2H_{CH_4}$ caused by methanotrophy

642 modeled with an α. value of 1.1353, or by oxidation with ·OH modeled with an α.value 1.294.

Preprints (www.preprints.org) | NOT PEER-REVIEWED | Posted: 29 October 2017 doi:10.20944/preprints201708.0009.v2

643 Other samples plot below and to the left of the shift caused by methanotrophy. Numbers represent
644 individual caves. Note that modeled cave air, represented by letters, generally plots left of the
645 theoretical oxidation lines. If error bars are not visible, they are smaller than the data points.

646

647

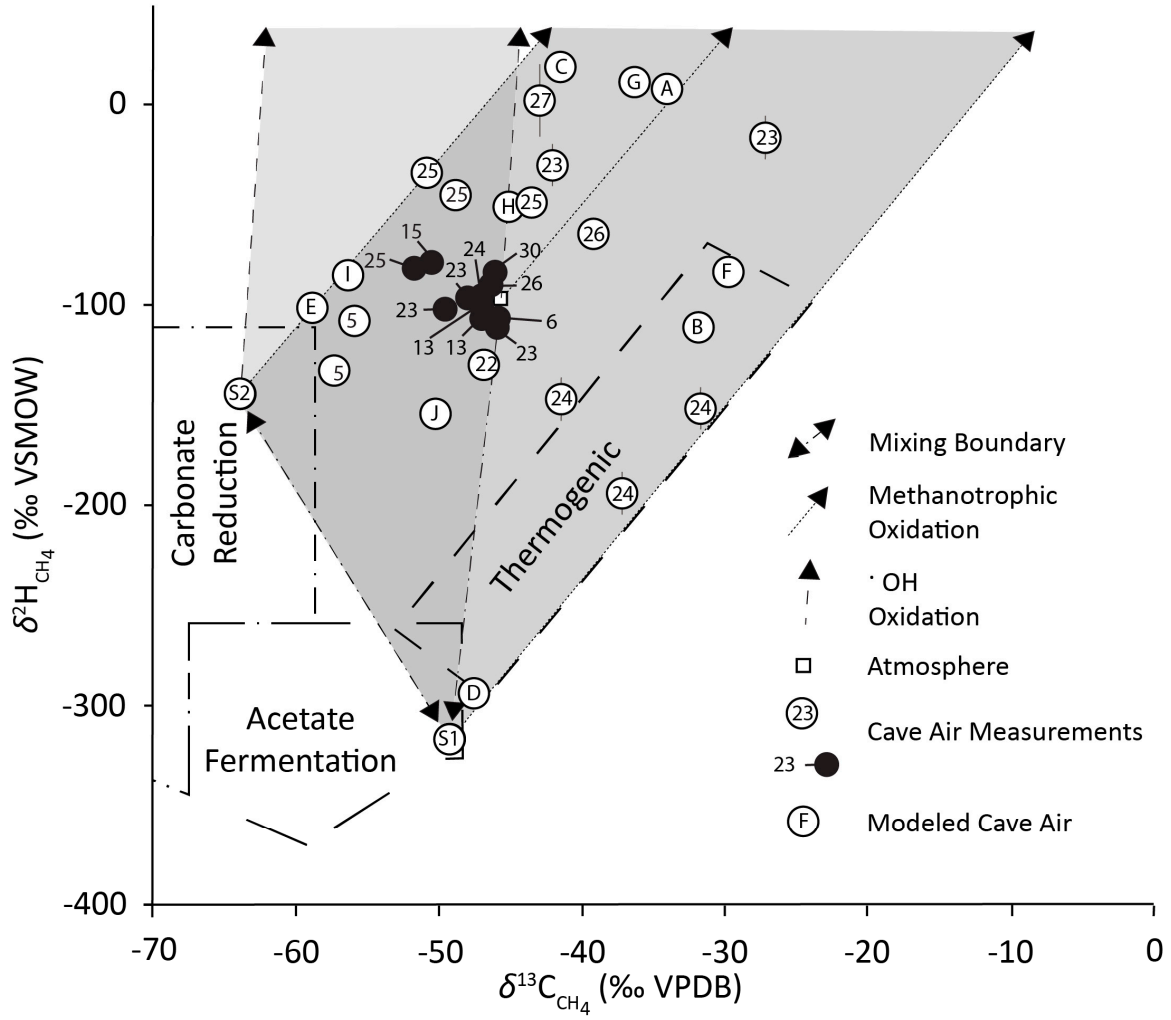

648

649 **Figure 7.** Stable isotopic composition of CH_4 in cave air samples plotted in $\delta^2H_{CH_4}$ *versus* $\delta^{13}C_{CH_4}$
650 space. CH_4 generated by carbonate reduction, acetate fermentation, and thermogenesis are plotted

Preprints (www.preprints.org) | NOT PEER-REVIEWED | Posted: 29 October 2017 doi:10.20944/preprints201708.0009.v2

within labeled fields (Whiticar, 1999). We model inputs from the atmosphere as (−47.5 ‰, −100 ‰, □), acetate fermentation as (−49 ‰, −325 ‰, S1), and carbonate reduction as (−63 ‰, −125 ‰, S2). Dotted lines indicate the expected shift in $\delta^2H_{CH_4}$ and $\delta^{13}C_{CH_4}$ caused by partial aerobic methane oxidation adopting a slope of 8.5. Dashed lines indicate the expected shift in $\delta^2H_{CH_4}$ and $\delta^{13}C_{CH_4}$ caused by oxidation with ·OH adopting a slope 75 (Saueressig et al., 2001; Feisthauer et al., 2011). Mixing in $\delta^2H_{CH_4}$ vs $\delta^{13}C_{CH_4}$ space plots as a straight line. Numbers represent individual caves. Note the all of the data points can be described by a source of CH_4 from the atmosphere, a source from acetoclastic fermentation (S1), a source from carbonate reduction (S2), mixing, and methanotrophic oxidation and do not plot within the bounds of ·OH oxidization. Error bars are not included with black circles for clarity. In other locations, if error bars are not visible, they are smaller than the data points.

Table 1: Overview of collected data. 'Discrete' measurements refer to the laboratory.

Cave	State	Collection date[a]	Sites measured	$[CH_4]$ min (ppmv)	$[CH_4]$ max (ppmv)	$[CO_2]$ min (ppmv)	$[CO_2]$ max (ppmv)	Methods
1	AL	2015-04-07	1	NA[b]	2.2	NA	378	*In-situ*
2	IN	2013-08-10	4	0.42	1.89	2140	8000	Discrete
3	IN	2013-08-07	3	0.23	4.2	13400	17900	Discrete
4	IN	2013-06-18	2	0.3	0.7	3900	5200	Discrete
5	IN	2013-06-29	3	0.4	1.18	3300	8600	Discrete
6	IN	2013-06-14	3	0.32	1.32	750	3700	Discrete
7	KY	2012-05-05	4	0.3	0.9	3500	6020	*In-situ*
8	KY	2012-05-06	5	0.1	0.4	5200	6200	*In-situ*
9	KY	2012-05-07	7	0.08	0.6	900	1500	*In-situ*
10	KY	2013-07-18	1	NA	1.79	NA	920	Discrete
11	KY	2013-07-18	1	NA	0.91	NA	2790	Discrete
12	KY	2013-07-18	1	NA	1.37	NA	1790	Discrete
13	KY	2015-04-10	4	2.3	2.6	349	390	Mixed
14	KY	2015-04-10	3	1.82	2.33	351	390	*In-situ*
15	KY	2015-04-10	2	0.9	1.8	440	486	Mixed
16	OH	2015-04-10	1	NA	1.95	NA	940	*In-situ*

Preprints (www.preprints.org) | NOT PEER-REVIEWED | Posted: 29 October 2017 doi:10.20944/preprints201708.0009.v2

17	PA	2013-07-15	5	1.4	1.9	1430	2400	Mixed
18	PA	2013-07-15	4	0.4	1.1	760	4250	Mixed
19	PA	2013-07-15	4	0.4	0.5	900	1400	Mixed
20	PA	2013-07-16	3	0.4	1.0	3390	4240	Mixed
21	TN	2013-07-18	3	0.5	1.25	2210	2430	Mixed
22	TN	2013-07-19	3	2.6	3.5	490	1610	Mixed
23	TN	2015-04-07	7	0.2	1.02	1100	1600	Mixed
24	TN	2015-04-08	6	0.6	1.6	1100	1515	Mixed
25	TN	2015-04-09	7	0.2	0.8	1430	2100	Mixed
26	TN	2015-04-09	3	0.6	0.79	630	660	Mixed
27	VA	2015-07-17	5	0.6	1.0	6300	14700	Mixed
28	VA	2015-07-17	4	0.4	0.8	2480	7600	Mixed
29	VA	2015-07-17	5	0.4	1.6	1100	8740	Mixed
30	VA	2015-07-18	5	0.3	1.5	1090	19900	Mixed
31	VA	2015-07-18	6	0.4	2.2	410	8900	Mixed
32	NZ[c]	2014-10-04	8	1.5	2.8	500	590	*In-situ*
33	NZ	2014-10-04	3	1.0	1.7	500	620	*In-situ*
34	NZ	2014-10-04	6	1.0	1.8	500	1000	*In-situ*
35	IN	2014-06-11	2	0.14	0.3	NA[d]	NA[d]	*In-situ*
36	MO	2016-09-24	9	0.1	1.5	2590	6190	*In-situ*

[a] Dates are formatted yyyy-mm-dd
[b] NA = not applicable where only 1 sample was obtained.
[c] NZ = New Zealand
[d] NA = Only CH_4 was measured

664

665

666 **Table 2:** *In-situ* instrumentation used in this study.

Instrument	Maker	Location	Method	Analytes Measured	Lower detection limits
GasFinder2	Boreal Laser	Spruce Grove, Alberta Canada	Tunable Diode Laser Spectroscopy	CH_4	1 ppmv m^{-1}
Inspectra	Gazomat, WEST Systems	Pontedera, Italy	Tunable Diode Laser Spectroscopy	CH_4	0.1 ppmv
LGD F200	Axetris, SARAD	Kägiswil, Switzerland	Tunable Diode Laser Spectroscopy	CH_4	0.2 ppmv
madIR-D01 CO2	Madur, SARAD	Zgierz, Poland	Tunable Diode Laser Spectroscopy	CO_2	400 ppmv

Preprints (www.preprints.org) | NOT PEER-REVIEWED | Posted: 29 October 2017 doi:10.20944/preprints201708.0009.v2

DX4030	Gasmet	Milton Keynes, United Kingdom	Fourier Transform Infrared Spectroscopy	CH_4, CO_2, NH_3,	0.3 ppmv CH_4, 200 ppmv CO_2, 0.1 ppbv NH_3
LI820	LICOR, WEST Systems	Pontedera, Italy	Nondispersive Infrared Spectroscopy	CO_2	5 ppmv
RTM 2200	SARAD	Dresden, Germany	Alpha spectroscopy	Rn	0 Bq/m³

667

668